Hydrogen-bond mediated transitional adlayer of glycine on Si(111)7×7 at room temperature

L. Zhang, A. Chatterjee, M. Ebrahimi, and K. T. Leung[a)]
WATLab and Department of Chemistry, University of Waterloo, Waterloo, Ontario N2L 3G1, Canada

(Received 18 December 2008; accepted 27 February 2009; published online 30 March 2009)

The growth of glycine film by thermal evaporation on Si(111)7×7 at room temperature has been studied by X-ray photoemission. In contrast to common carboxylic acids, glycine is found to adsorb on Si(111)7×7 dissociatively through cleavage of a N–H bond instead of O–H bond. The intricate evolution of the observed N 1*s* features at 399.1, 401.4, and 402.2 eV with increasing film thickness demonstrates the existence of a transitional adlayer between the first adlayer and the zwitterionic multilayer. This transitional adlayer is estimated to be 1–2 adlayer thick and is characterized by the presence of intermolecular N···HO hydrogen bond. An intramolecular proton transfer mechanism is proposed to account for the adsorption process through the amino group. © *2009 American Institute of Physics*. [DOI: 10.1063/1.3106762]

I. INTRODUCTION

Thin films of amino acids evaporated in ultrahigh vacuum on well-defined solid surfaces have been studied extensively by a number of techniques, including X-ray photoelectron spectroscopy (XPS), scanning tunneling microscopy (STM), and thermal desorption spectrometry.[1–10] These studies focus specifically on interfacial bonding, conformation, thermal stability, self-assembly, and chirality of the amino acid films on various metal and oxide substrates. With the amino ($-NH_2$) and carboxyl (–COOH) groups in common, different amino acids ($NH_2CHRCOOH$) are identified by their unique side chains (*R*). As the building blocks of peptides and proteins, amino acids, glycine in particular (with *R* being the H atom), are intensively studied to provide the fundamental reference information for more complicated proteins and peptides. It is well known that glycine exists as neutral molecule (NH_2CH_2COOH) in the gas phase and as zwitterion ($NH_3^+CH_2COO^-$) in solids and solutions, while deprotonated or anionic ($NH_2CH_2COO^-$) and protonated or cationic ($NH_3^+CH_2COOH$) forms are commonly found in solutions. When glycine is evaporated onto a substrate, the prevailing form is found to depend on the nature and temperature of the substrate and the film thickness. A thick (multilayer) glycine film always exists in the zwitterionic form regardless of the substrates, while the other forms could occur in thin films due to the interactions between glycine and the substrates that inhibit proton transfer among glycine molecules. Low substrate temperature or an inert substrate would therefore favor the formation of zwitterions even for thin films due to reduced interactions with the substrates. For example, glycine was found to adsorb in the zwitterionic form on Pt(111) (Ref. 1) at low temperature (<250 K) and on Au(111) at room temperature (RT),[2] but as the anionic form on Cu(110) (Refs. 3–5) and Cu foil[6] at RT. For NiAl(110) (Ref. 7) and Al_2O_3-film substrates,[8] glycine adsorbs in both the zwitterionic form at low temperature (<250 K) and anionic form at RT.

Most of the earlier studies on glycine adsorption on different substrates mainly focus on the thin-film (monolayer) and thick-film (multilayer) regimes. However, the transition from monolayer to multilayer is not well understood. This intermediate regime is especially important for investigating the chemical bonding involved in the evolution from the chemisorbed state to the zwitterionic form. Depending on the nature and temperature of the substrate, glycine could bond to the substrate in several ways: (a) through the N lone pair of the amino group,[4] (b) with the N atom after one N–H bond cleavage,[10] (c) with one of the O atoms in unidentate coordination, or (d) with both O atoms in bidentate or bridging coordination after O–H bond cleavage.[3–6,9] In the present work, we report a detailed photoemission study of the growth evolution of glycine on Si(111)7×7 with focus on this intermediate regime. In addition to its obvious practical interest as a semiconductor surface, the 7×7 surface offers unique electronic and surface structures with directional dangling-bond sites[11] for understanding the fundamental interactions involved in organosilicon chemistry. We demonstrate, for the first time, the presence of a transitional adlayer between the interfacial (first) adlayer and the zwitterionic multilayer film. The N 1*s* spectra reveal that the interfacial adlayer bonds to the 7×7 surface through the N atom by N–H bond cleavage, while the transitional adlayer involves N···HO hydrogen bonding. The presence of hydrogen bonding in the transitional adlayer suggests its viability as a reversible platform for linking with other biomolecules by their hydrogen bonding interactions, thereby providing a versatile method for biofunctionalization of the Si surface.[12]

II. EXPERIMENTAL DETAILS

The experiments were performed in a custom-built five-chamber ultrahigh vacuum system (Omicron Nanotechnology, Inc.), with the base pressure better than 5×10^{-11} Torr.

[a)]Author to whom correspondence should be addressed. Electronic mail: tong@uwaterloo.ca.

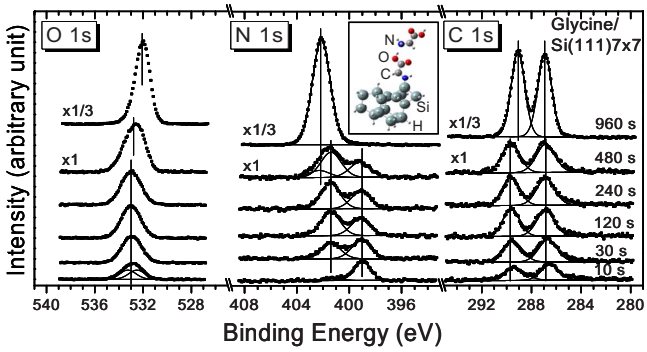

FIG. 1. (Color online) XPS spectra of the C 1*s* (right), N 1*s* (center), and O 1*s* regions (left) of glycine on Si(111)7×7 as a function of deposition time. The inset shows the optimized geometry of a N-bonded glycine adstructure coupled to a second glycine molecule through an O–H···N hydrogen bond on a $Si_{16}H_{18}$ model surface, obtained by a DFT/B3LYP calculation with a 6-31++G(*d*,*p*) basis set.

The analysis chamber was equipped with a SPHERA hemispherical electron analyzer and a monochromatized Al $K\alpha$ (1486.7 eV) X-ray source for XPS, and a variable-temperature scanning probe microscope (SPM) for atomic resolution imaging. Single-side polished Si(111) chips (11 ×2 mm^2, 0.3 mm thick), with a resistivity of 0.005 Ω cm (Virginia Semiconductors), were cleaned by first outgassing at 400 °C overnight, followed by flash annealing at 1200 °C several times (by direct-current heating), until no C contaminants were detectable by XPS and large-area terraces with the 7×7 reconstruction were observed by SPM. Glycine (with a normal melting point of 182 °C) was deposited onto the Si substrates by thermal evaporation using a water-cooled effusion cell (designed specially for organic materials evaporation) in a separate sample preparation chamber. During evaporation, the temperature of the effusion cell was kept at 140 °C, leading to a partial pressure of 5.0×10^{-9} Torr for the 30 amu mass fragment (corresponding to the base ion $NH_2CH_2^+$ of glycine), as registered by a quadrupole mass spectrometer. In the present work, glycine was deposited sequentially onto the Si substrate held at RT. The amount of glycine deposition was indicated by the total deposition time, which can be used to provide a measure of the relative film thickness. After each deposition, the Si 2*p*, O 1*s*, N 1*s*, and C 1*s* core-level spectra were measured with a pass energy of 20 eV, which gave an effective linewidth of 0.8 eV full width at half maximum (FWHM) for the Ag $3d_{5/2}$ photoline at 368.3 eV. For each deposited glycine film, the energy scale was referenced to the Si $2p_{3/2}$ photoline (99.3 eV) of the substrate. The spectra were fitted with Gaussian–Lorentzian line shapes after appropriate background removal by using the CASA-XPS software.

III. RESULTS AND DISCUSSION

Figure 1 shows the C 1*s*, N 1*s*, and O 1*s* spectra of glycine films with different thicknesses, as represented by the deposition time. For the lowest exposure of 10 s, the N 1*s* spectrum (center panel) exhibits a dominant feature at 399.1 eV attributed to N–Si bond, in good accord with the N 1*s* features at 398.8–399.4 eV found for dissociative adsorption of amines (e.g., hexylamine and *N*-methylpentylamine) via the N–H bond cleavage on Si(100)2×1 and Si(111)7×7 at RT.[13–16] Further deposition to 30 s leads to saturation of the feature at 399.1 eV and the emergence of a new feature at 401.4 eV, which gradually increases in intensity at 120 s deposition and becomes saturated at 240 s deposition with the saturation intensity about 1.5 times that of the feature at 399.1 eV. At the 480 s deposition, a new feature appears at 402.2 eV, with the intensities of both features at the lower binding energy remaining nearly unchanged, and it becomes the only prominent feature for the 960 s and longer deposition times. The binding energy of this feature agrees with that of the protonated amino group (NH_3^+).[1,8,10,17] Given that the corresponding binding energy of the O 1*s* spectrum for the 960 s deposition is found to be consistent with that of carboxylate (COO^-) (see below), this glycine film exists predominantly in the zwitterionic form, as expected for glycine in the bulk state.

The new N 1*s* feature observed at 401.4 eV has not been reported for glycine in literature. In an early study by Clark *et al.*[17] on a series of glycine and their peptides (in powder form), the N 1*s* feature for a neutral amino group ($-NH_2$) was found to be generally located at 400.4 eV, i.e., 1.8 eV lower than that for $-NH_3^+$ found in the zwitterions. The feature at 401.4 eV therefore corresponds to a new N species that is more positively charged than that in NH_2 but less so than that in NH_3^+ . Here it is reasonable to assume that the final state relaxation and screening effects are similar for different N species of the glycine film on Si(111)7×7.[18] We attribute this feature to N involved in the N···H–O hydrogen bonding with the carboxyl group of another glycine molecule. Similar N···H–O hydrogen bonding has been reported by O'Shea *et al.*[19] in the adsorption of isonicotinic acid (pyridine-4-carboxylic acid) on TiO_2(110), where the N in the pyridine ring of one molecule forms a hydrogen bond with the carboxyl group of another molecule in the layer above. The 1*s* binding energy of the N atom involved in the hydrogen bond (407.0 eV) is 1.7 eV higher than that without hydrogen bonding in isolated pyridine (405.3 eV). The larger N 1*s* core-level shift induced by hydrogen bonding for isonicotinic acid (1.7 eV) than that for glycine (1.0 eV) [this value was calculated by using the N 1*s* binding energy for the hydrogen bonding feature (401.4 eV) and that for neutral glycine molecules (400.4 eV) reported by Clark *et al.*[17]] is due to their different N local chemical environments. Using density functional theory (DFT) calculation, O'Shea *et al.*[19] further illustrated that the strength of the hydrogen bonding interaction (and therefore the core-level shift) could increase with increasing molecular cluster size due to a process known as cooperative hydrogen bonding.

Owing to the directionality and selectivity, hydrogen bonding has also been used to account for self-assembly of small organic molecules on well-defined substrates as observed by STM, including, e.g., pairs and double rows of cysteine on Au(110),[20,21] L-methionine nanogratings on Ag(111),[22] 4-[*trans*-2-(pyrid-4-yl-vinyl)]benzoic acid (PVBA) chains on Ag(111),[23] and hexagonal network of melamine and perylene tetracarboxylic di-imide on Ag/Si(111)-($\sqrt{3}\times\sqrt{3}$)*R*30°.[24] Intermolecular hydrogen bonding was also proposed to explain the "(3×2)pg" low

energy electron diffraction pattern observed for glycinate on a Cu(110) surface.[25] Among neutral glycine molecules, hydrogen bonding can occur in two possible configurations shown in the following schemes: (a) a head-to-head configuration between the carboxyl groups to form double O–H···O hydrogen bonds as in cysteine pairs on Au(110) (Ref. 20), and (b) a head-to-tail configuration between the carboxyl and amino groups (O–H···N or N–H···O) as in PVBA chains on Ag(111).[23]

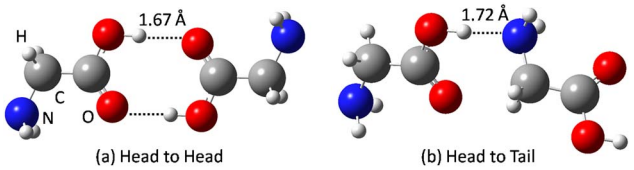

We therefore assign the N 1*s* feature at 401.4 eV observed in the present work to an O–H···N head-to-tail hydrogen bonding configuration, which may form between the first adlayer (interfacial layer) and the second and possibly third adlayers (transitional layer). A "transitional region" has been noted in the earlier thermal desorption profiles of glycine films on Pt(111) (Ref. 1) and Ni foil.[26] The N 1*s* spectral evolution with the deposition time in the present work clearly reveals three different growth stages of glycine on Si(111)7×7: (1) formation of the covalently bonded interfacial layer, (2) development of the hydrogen-bonded transitional layer, and (3) continuous growth of the zwitterionic multilayer.

In the inset of Fig. 1, we show a schematic diagram of the N-bonded glycine adstructure coupled to a second glycine molecule through an O–H···N head-to-tail hydrogen bond on a modeled Si surface. The electronic structure calculation was performed by using the GAUSSIAN 03 software. A $Si_{16}H_{18}$ cluster[27] was used to represent the restatom-adatom sites at the faulted half of the Si(111)7×7 unit cell after adopting the dimer-adatom-stacking fault model of Takayanagi *et al.*[11] All geometries including the $Si_{16}H_{18}$ cluster and plausible glycine adstructures were optimized by using the DFT method with the B3LYP hybrid functional[28,29] and 6-31++G(*d*,*p*) basis set, and no imaginary frequencies were found in the corresponding frequency calculations. Evidently, bonding to the Si adatom is found to give a more stable equilibrium geometry than bonding to the restatom. The calculated bond length for the O–H···N hydrogen bond (1.89 Å) is found to be in general accord with that expected of a typical hydrogen bond (1.6–2.0 Å). Furthermore, the calculated N 1*s* orbital energy for the hydrogen-bonded glycine (419.5 eV), representing the transitional adlayer, is higher than that for the N-bonded glycine (418.5 eV), representing the interfacial layer. Within the limit of Koopmans' theorem,[30] this ordering of calculated orbital energies is in good accord with that of the corresponding observed N 1*s* binding energies, which provides further support for our spectral assignment of the N 1*s* features.

Figure 1 also shows the evolution of the corresponding O 1*s* spectra of the glycine film with increasing deposition time (left panel). Both the position (533.0 eV) and the width (1.9 eV FWHM) of the O 1*s* peak appear to be unchanged for deposition up to 240 s, indicating similar chemical environments of the O atoms in the interfacial and transitional layers. Given that a large O 1*s* chemical shift of 1.3 eV to the higher binding energy has been observed for formic acid from chemisorbed (formate in a unidentate configuration) to physisorbed states,[31] the single-peak O 1*s* feature therefore rules out the formation of O–Si covalent bonds in the interfacial layer. For the 10 s deposition, we fitted the corresponding O 1*s* spectrum (of the nonbonded carboxylic acid group) with two components of equal intensity and width at 532.5 and 533.3 eV, corresponding to the carbonyl O (C=O) and the hydroxyl O (OH), respectively. These binding energies are in good accord with those of carbonyl O (532.0 eV) and of hydroxyl O (533.3 eV) of mercaptopropionic acid bonded through the S end on Au(111).[32] The present assignment of the lower binding energy (532.5 eV) to carbonyl O is also in good agreement with that in acetaldehyde and acetone (532.7 eV) (Ref. 33) and in 3,4,9,10-perylene tetracarboxylic dianhydride (532.4 eV).[34] For the 480 s deposition, the corresponding O 1*s* peak becomes asymmetric and appears to be shifting to the lower binding energy side. Further deposition to 960 s leads to a much sharper O 1*s* peak (1.45 eV FWHM) and a lower binding energy position of 532.1 eV, which suggests that the O atoms in the multilayer film have a more homogeneous chemical environment and are more negatively charged. The observed binding energy position corresponds to that of carboxylate,[1] reflecting the zwitterionic nature of the multilayer film.

Figure 1 (right panel) shows that for deposition up to 480 s, the C 1*s* spectra reveal two well-defined peaks at 286.9 and 289.7 eV, corresponding to, respectively, methylene ($>CH_2$) and carboxyl C,[8] with their intensity ratio (1:1) found to be in good accord with their stoichoimetry. For the 960 s deposition, a notable shift in the carboxyl C 1*s* peak to the lower binding energy by 0.6 eV is found, while the location of the methylene C 1*s* peak remains unchanged. A similar binding energy shift in the corresponding O 1*s* has been discussed previously. These shifts found for the multilayer are consistent with the presence of a delocalized negative charge over the carboxylate group of the zwitterions, in contrast to the carboxyl group of the N-bonded adstructure (in the transitional and interfacial layers). The resulting energy separation between these two C 1*s* peaks found for the multilayer (2.2 eV) is in good accord with that for the glycine zwitterionic multilayers found on other substrates.[1,4,8] Conversely, the larger energy separation found for the shorter deposition time (2.8 eV) therefore confirms the nonzwitterionic nature of the interfacial and transitional layers.

The adsorption properties of glycine on Si(111)7×7 and Si(100)2×1 are found to be quite different. In particular, instead of the formation of O–Si bonds from O–H bond dissociation in glycine on Si(100)2×1 as observed by Lopez *et al.*[9] and calculated by Qu *et al.*,[35] formation of N–Si bonds as a result of N–H dissociative adsorption of glycine on Si(111)7×7 is found. As shown in Fig. 2, based on the electrophilic-nucleophilic consideration,[36,37] the formation of a dative bond between the electron-deficient Si adatom and the N lone pair (structure I) is more favorable than that between the adatom and the O lone pair. Hydrogen abstraction from a dative-bonded adduct can occur directly by an

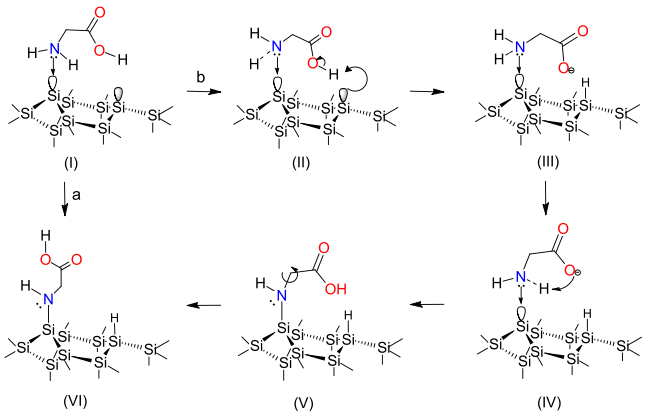

FIG. 2. (Color online) Proposed (a) direct and (b) indirect proton transfer mechanisms for the formation of N-bonded glycine (in the first adlayer) on an adatom-restatom model surface of Si(111)7×7.

electron-rich Si restatom (pathway a) or indirectly via an intramolecular proton transfer (pathway b). Given that the separation between the N and O atoms in glycine (2.8 Å) is compatible with the adatom-restatom separation (4.6 Å),[37] the restatom can abstract a proton from the OH group (structure II), producing a temporary negatively charged carboxylate species (structure III), which would undergo an intramolecular proton transfer from the amino group (structure IV) to produce structure V and to structure VI upon rotation around the C–N bond axis. Because the N–H bond distance (1.01 Å) is considerably shorter than the adatom-restatom separation (4.6 Å), the direct proton transfer (pathway a) is expected to be less favorable than the indirect pathway (pathway b) on the Si(111)7×7 surface. In the case of Si(100)2×1, the corresponding separation between the electron-rich up-atom and electron-deficient down-atom of the Si dimer (2.3 Å) is compatible with both the N–H (1.01 Å) and O–H bond lengths (0.91 Å) for direct H abstraction. Indeed, the DFT calculation of glycine on Si(100)2×1 by Qu *et al.*[35] showed that O–H bond dissociation has a lower activation barrier than the N–H bond dissociation, which leads to exclusive unidentate O bonded product. It should be noted the bidentate adstructure of glycine through O–H and N–H dissociation on the two adatoms of the Si(111)7×7 proposed by Huang *et al.*[10] is not physically possible due to the large separation between the adatom and its nearest adatom neighbor (6.65 Å) compared to the O-to-N separation in glycine (2.8 Å).

IV. CONCLUSIONS

We have studied the growth of glycine on Si(111)7×7 at RT in ultrahigh vacuum by XPS. Three N 1*s* features at 399.1, 401.4, and 402.2 eV emerge sequentially with increasing deposition time, which indicates three distinct stages in the growth process. Initially, glycine undergoes N–H dissociation to form a N-bonded adstructure at the surface, followed by the formation of a transitional layer (1–2 adlayer thick), which is characterized by the presence of the intermolecular O–H···N hydrogen bonding. Continued deposition gives rise to multilayers with glycine in the zwitterionic form. The evolution of the O 1*s* and C 1*s* features with the deposition time also supports this growth model. An intramolecular proton transfer mechanism has been proposed to account for the adsorption process through the amino group. The present observation of intermolecular N···H–O hydrogen bonding in amino acid, for the first time by XPS, has opened up a new way of detecting surface hydrogen bonds. Our preliminary study[12] further shows that the transitional layer can also be formed not only between the adsorbed glycine layer (the first adlayer) and other biomolecules with an amino group (e.g., glycylglycine and adenine) but also reversibly, potentially providing a facile way to change the surface reactivity and selectivity of the biomolecular functionalized Si surface.

ACKNOWLEDGMENTS

This work was supported by the Natural Sciences and Engineering Research Council of Canada.

[1] P. Lofgren, A. Krozer, J. Lausmaa, and B. Kasemo, Surf. Sci. **370**, 277 (1997).
[2] X. Y. Zhao and J. Rodriguez, Surf. Sci. **600**, 2113 (2006).
[3] S. M. Barlow, K. J. Kitching, S. Haq, and N. V. Richardson, Surf. Sci. **401**, 322 (1998).
[4] J. Hasselstrom, O. Karis, M. Weinelt, N. Wassdahl, A. Nilsson, M. Nyberg, L. G. M. Pettersson, M. G. Samant, and J. Stohr, Surf. Sci. **407**, 221 (1998).
[5] M. Nyberg, J. Hasselstrom, O. Karis, N. Wassdahl, M. Weinelt, A. Nilsson, and L. G. M. Pettersson, J. Chem. Phys. **112**, 5420 (2000).
[6] K. Uvdal, P. Bodo, A. His, B. Liedberg, and W. R. Salaneck, J. Colloid Interface Sci. **140**, 207 (1990).
[7] G. Tzvetkov, M. G. Mamsey, and F. P. Netzer, Surf. Sci. **526**, 383 (2003).
[8] G. Tzvetkov, G. Koller, Y. Zubavichus, O. Fuchs, M. B. Casu, C. Heske, E. Umbach, M. Grunze, M. G. Mamsey, and F. P. Netzer, Langmuir **20**, 10551 (2004).
[9] A. Lopez, T. Heller, T. Bitzer, and N. V. Richardson, Chem. Phys. **277**, 1 (2002).
[10] J. Y. Huang, Y. S. Ning, K. S. Yong, Y. H. Cai, H. H. Tang, Y. X. Shao, S. F. Alshahateet, Y. M. Sun, and G. Q. Xu, Langmuir **23**, 6218 (2007).
[11] K. Takayanagi, Y. Tanishiro, and S. Takahashi, J. Vac. Sci. Technol. A **3**, 1502 (1985).
[12] L. Zhang, A. Chatterjee, and K. T. Leung (unpublished).
[13] X. P. Cao and R. J. Hamers, J. Vac. Sci. Technol. B **20**, 1614 (2002).
[14] X. P. Cao and R. J. Hamers, Surf. Sci. **523**, 241 (2003).
[15] X. P. Cao and R. J. Hamers, J. Am. Chem. Soc. **123**, 10988 (2001).
[16] X. P. Cao, S. K. Coulter, M. D. Ellison, H. B. Liu, J. M. Liu, and R. J. Hamers, J. Phys. Chem. B **105**, 3759 (2001).
[17] D. T. Clark, J. Peeling, and L. Colling, Biochim. Biophys. Acta **453**, 533 (1976).
[18] N. Martensson and A. Nilsson, J. Electron Spectrosc. Relat. Phenom. **75**, 209 (1995).
[19] J. N. O'Shea, J. Schnadt, P. A. Bruhwiler, H. Hillesheimer, N. Martensson, L. Patthey, J. Krempasky, C. K. Wang, Y. Luo, and H. Agren, J. Phys. Chem. B **105**, 1917 (2001).
[20] A. Kuhnle, T. R. Linderoth, B. Hammer, and F. Besenbacher, Nature (London) **415**, 891 (2002).
[21] A. Kuhnle, L. M. Molina, T. R. Linderoth, B. Hammer, and F. Besenbacher, Phys. Rev. Lett. **93**, 086101 (2004).
[22] A. Schiffrin, A. Riemann, W. Auwarter, Y. Pennec, A. Weber-Bargioni, D. Cvetko, A. Cossaro, A. Morgante, and J. V. Barth, Proc. Natl. Acad. Sci. U.S.A. **104**, 5279 (2007).
[23] J. V. Barth, J. Weckesser, C. Z. Cai, P. Gunter, L. Burgi, O. Jeandupeux, and K. Kern, Angew. Chem., Int. Ed. **39**, 1230 (2000).
[24] J. A. Theobald, N. S. Oxtoby, M. A. Phillips, N. R. Champness, and P. H. Beton, Nature (London) **424**, 1029 (2003).
[25] M. Nyberg, M. Odelius, A. Nilsson, and L. G. M. Pettersson, J. Chem. Phys. **119**, 12577 (2003).
[26] D. Holtkamp, M. Jirikowsky, M. Kempken, and A. Benninghoven, J.

Vac. Sci. Technol. A **3**, 1394 (1985).
[27] F. Bournel, S. Carniato, G. Dufour, J.-J. Gallet, V. Ilakovac, S. Rangan, and F. Rochet, Phys. Rev. B **73**, 125345 (2006).
[28] A. D. Becke, J. Chem. Phys. **98**, 5648 (1993).
[29] C. Lee, W. Yang, and R. G. Parr, Phys. Rev. B **37**, 785 (1988).
[30] T. C. Koopmans, Physica (Amsterdam) **1**, 104 (1934).
[31] J. Y. Huang, H. G. Huang, K. Y. Lin, Q. P. Liu, Y. M. Sun, and G. Q. Xu, Surf. Sci. **549**, 255 (2004).
[32] C. M. Whelan, J. Ghijsen, J. Pireaux, and K. Maex, Thin Solid Films **464–465**, 388 (2004).
[33] J. L. Armstrong, J. M. White, and M. Langell, J. Vac. Sci. Technol. A **15**, 1146 (1997).
[34] T. Soubiron, F. Vaurette, J. P. Nys, B. Grandidier, X. Wallart, and D. Stievenard, Surf. Sci. **581**, 178 (2005).
[35] Y. Q. Qu, Y. Wang, J. Li, and K. L. Han, Surf. Sci. **569**, 12 (2004).
[36] C. Mui, J. H. Han, G. T. Wang, C. B. Musgrave, and S. F. Bent, J. Am. Chem. Soc. **124**, 4027 (2002).
[37] F. Tao and G. Q. Xu, Acc. Chem. Res. **37**, 882 (2004).